We are IntechOpen,
the world's leading publisher of
Open Access books
Built by scientists, for scientists

4,800
Open access books available

122,000
International authors and editors

135M
Downloads

Our authors are among the

154
Countries delivered to

TOP 1%
most cited scientists

12.2%
Contributors from top 500 universities

BOOK CITATION INDEX
CLARIVATE ANALYTICS
INDEXED

WEB OF SCIENCE™

Selection of our books indexed in the Book Citation Index
in Web of Science™ Core Collection (BKCI)

Interested in publishing with us?
Contact book.department@intechopen.com

Numbers displayed above are based on latest data collected.
For more information visit www.intechopen.com

Osmotic Properties of Polysaccharides Solutions

Kruk Joanna, Pancerz Michał and Ptaszek Anna

Additional information is available at the end of the chapter

Abstract

Osmotic properties of polysaccharides' solutions and associated biopolymer-solvent and biopolymer-biopolymer type interaction are very important from a technological point of view. The knowledge of osmotic properties of these systems provides the basis to appropriate use of polysaccharides having comply with the relevant technology functions, impart the appropriate texture and forming the sensory properties of the final product. Furthermore, an important issue is the effect of time on the osmotic properties of polysaccharides', because with time, the aforementioned effects may change. Membrane osmometry is one of the methods used in the studies of synthetic polymers to determine their average molecular mass and the degree of interaction between a polymer and a solvent. This method is successfully applied in the case of biopolymers that include polysaccharides. The existence of the osmotic pressure, formed by diffusion of solvent molecules through a semi-permeable membrane, is the basis of this method. Analysis and interpretation of osmometric research results is based on the van't Hoff equation dependency of the concentration. The second virial coefficient obtained based on this relation allows characterisation of biopolymer-solvent interactions, and thus biopolymer tendency to solvation. The third virial coefficient provides information on mutual interactions between the biopolymer molecules, as well as its tendency to aggregate.

Keywords: osmotic pressure, virial coefficient, overlap concentration

1. Introduction

Osmotic properties are part of wider group of colligative phenomena and concern the liquid-vapour equilibrium in multi-component systems. This group of colligative properties includes depression of the freezing point (cryoscopy), boiling point elevation (ebullioscopy) and osmotic pressure in general. The osmotic pressure can be associated with water activity of
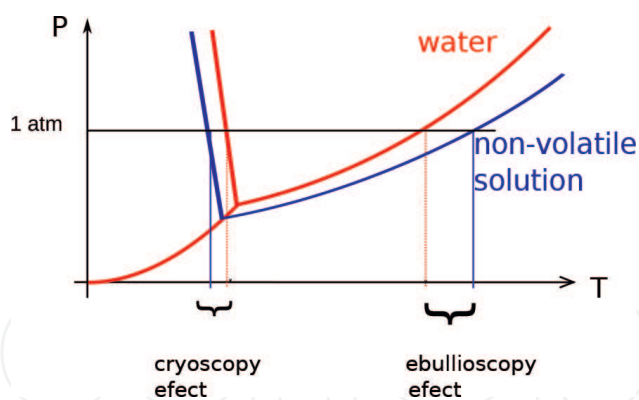
Figure 1. Phase equilibrium for pure water and solution.

various types of products. The essence of the discussed phenomena is related to the changes of pressure of the saturated vapour (**Figure 1**), which causes the dissolution of the non-volatile substance.

If the non-volatile substance is a low-molecular-weight chemical compound, the changes in the vapour pressure can be explained by common phenomena, such as association or solvation, which are a result of interactions between molecules. The difference of the vapour pressure would in this case be directly proportional to the molecular mass of a dissolved substance. The osmotic measurements can therefore be used to determine the molar mass, or for multi-molecular substances with significant polydispersion, to determine the average osmotic molec-ular mass. The osmosis process takes place between the solution and a clear solvent, or between solutions of different concentrations, provided they are separated by a membrane, which is permeable only to the solvents molecules (**Figure 2**). The solvent moves through the membrane from the solution with lower concentration of the dissolved substance (or from the area of clear solvent) towards the solution with higher concentration. From the point of view of the molecules present in the solution, it is a phenomenon opposite to diffusion. From the solvents perspective, it is a natural intent to balance the chemical potentials, which results in the dilution of the solution with higher concentration. If the osmotic equilibrium takes place in
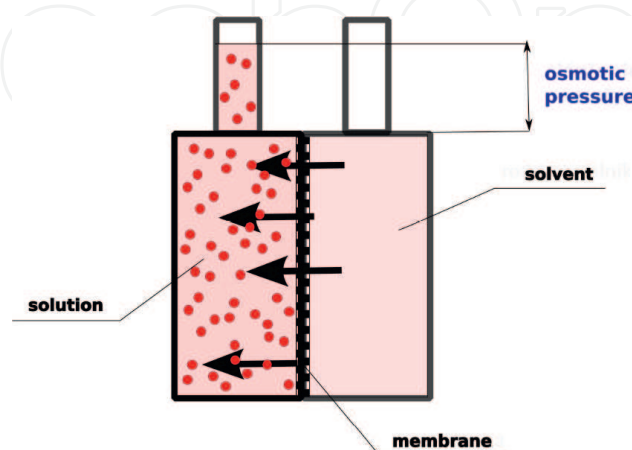

Figure 2. Osmosis mechanism.

a solution-clear solvent system, the dilution of the solution becomes so significant that the dissolved substances presence becomes suppressed and as a result, the pressure of solvents vapours over the solution becomes equal to the vapour pressure over the clear solvent. Because of that, the osmotic pressure is considered as one of the colligative processes.

2. Measurements of osmotic properties

The measurements of osmotic pressure can be carried out using two types of osmometers: membrane and vapour (**Figure 3**).

A membrane osmometer consists of two chambers divided by a membrane with specific pore sizes, which allow the solvent to move. One of the chambers is filled with pure solvent, while the other with the studied solution and the difference in the hydrostatic pressure between the two chambers is measured. These devices can be used to determine the pressure up to about 0.1 mmH_2O, which in practice means measuring polymer and biopolymer solutions of up to 2000 kDa. The lower measuring range depends on the membrane's permeability. In the case of these devices, the membrane itself is the source of the main issues. The membrane's permeability depends on its structure: whether it has a system of pores (inorganic materials) or is a molecular sieve (organic materials). Permeability is usually expressed by the lowest molecular mass of a substance that the membrane allows through (*cut-off* value). For biopolymer solutions characterised by high polydispersion, there is a possibility of diffusion of fractions with lower molecular mass through the membrane. If it is close to the solvent's molecular mass, the obtained value of osmotic pressure is not affected. The solvent's flow through the membrane can cause a so-called *balloon effect*, manifested by bulging of the membrane and distortion of its surface, which can affect its properties. Another issue is caused by the viscosity effect of the solution, which for biopolymers forming structural fluids, even at their low concentrations,
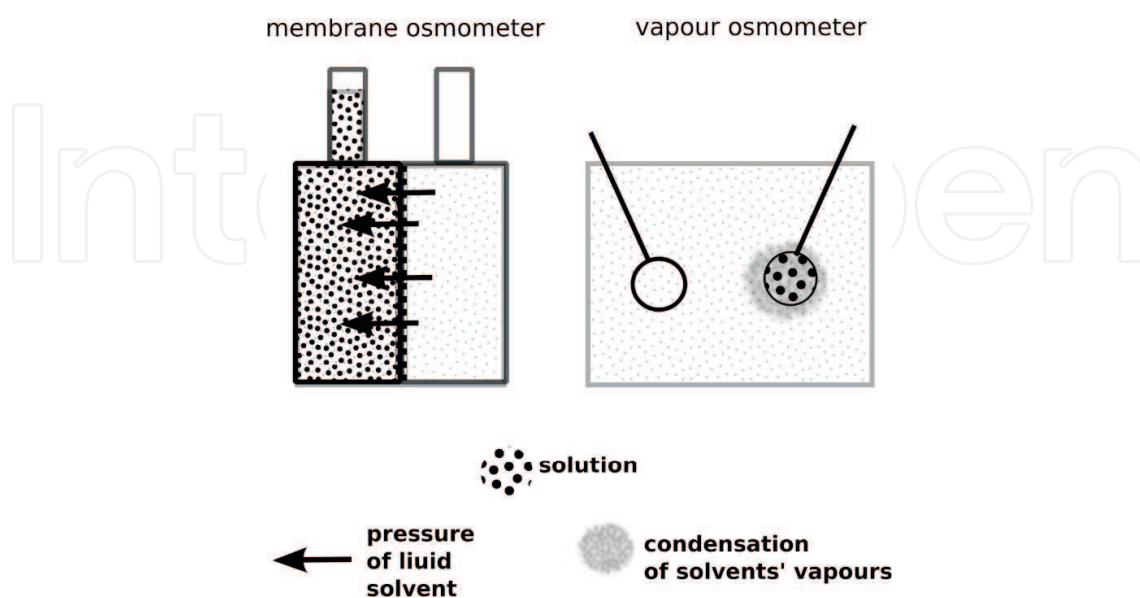

Figure 3. Types of osmometers.

can negatively affect the measurements due to the long time required for the establishment of osmotic equilibrium. Reaching the equilibrium is directly related to the solvent molecules diffusion throughout the solution. The vapour osmometer operates on a different premise: it measures the heating effect of the condensation of solvent's vapour on the drop of the tested solution, as well as a clear solvent. The osmometer consists of a chamber filled with the solvents vapours, in which two capillaries are placed (**Figure 3**). The capillaries are filled with the solvent and the tested solution, respectively, in such a way that drops form on their ends. In a state of thermodynamic equilibrium, the rate of solvent's evaporation and the rate of the condensation of its vapours would be the same. The whole process is carried out at a characteristic temperature—the boiling point (at a given pressure). On the other side, an intensive condensation of the solvent's vapours on the solution drop occurs, caused by the difference of the vapour pressure, which results in a local increase of temperature in the near vicinity of the drop (compared to the boiling temperature of pure solvent). It is that difference of temperatures, that is, the basis of the measurements in the vapour osmometer. Devices of this type can be used to carry out measurements of molecular masses in the range from 40 to 40 kDa. For these devices, one of the limitations is the viscous effect of the tested solution, which for biopolymers plays a significant role. Moreover, the measurement range of these devices makes them practically impossible to use to study multi-molecular substances.

3. Osmotic equilibrium equation

The test results obtained from the osmotic pressure measurements are analysed based on the virial equation, which is mainly associated with real gases. While it might seem surprising, the validity of this approach is based on the nature of interactions between molecules, which move chaotically and collide with each other. In the real gases, the collisions between molecules are not elastic, and as a consequence, they shape the characteristics of the gas phase, so that they diverge from the Clapeyron's law. For liquid solutions, a similar interpretation can be applied: the polymer/biopolymer molecules are incomparably larger than the solvent molecules (colloid solutions), and therefore, the solvent becomes the `background' for the interactions between macromolecules. For a macromolecule-solvent system, the nature of the interactions is more complex. Numerous studies on the structure of macromolecules in solutions indicate to two possible behaviour patterns, dependent on the interactions between the solvent and the polymer/biopolymer chains (**Figure 4A**). As a result of those interactions, the polymer chain can undergo either expansion or contraction (collapse). The scenario is decided by the affinity to the solvent. The chain's expansion is related to the absorption of the solvents molecules in between the chain's segments and can be caused by solvation, electrostatic (Couloumb) interactions, formation of a helical structure or the presence of a spatial hindrance in the case of branched polymers (**Figure 4A**). A contraction caused by low affinity to the solvent induces a collapse, which is often accompanied by the aggregation of the chains or creation of a rigid branched structure, which leads to phase separation (**Figure 4A**).

The quality of a solvent is examined in close relation to a specific polymer/biopolymer. A good solvent (**Figure 4B**) causes the expansion of the chain in the solution, which in the range of
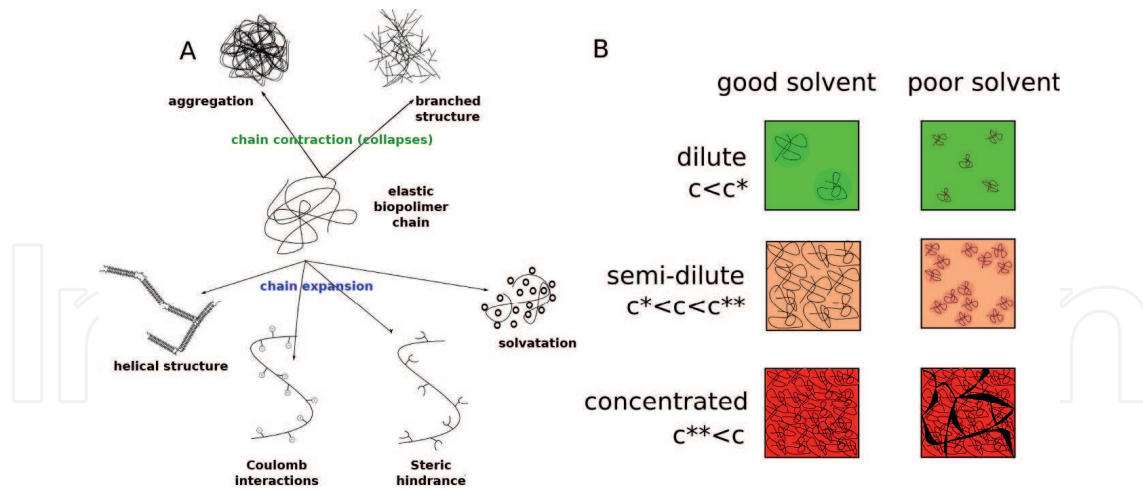
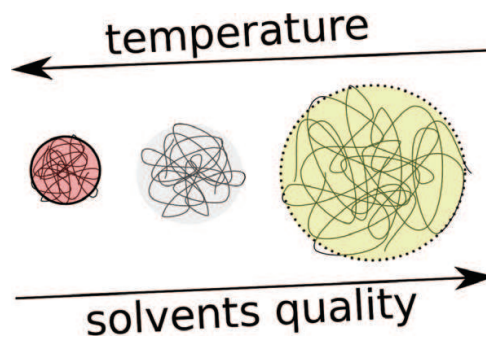**Figure 4.** Swelling mechanism (A) and quality of solvent (B).

Figure 5. Swelling as a function of temperature and solvents quality.

concentrations $c < c^*$ (diluted solution) can undisturbedly interact with the solvent. Exceeding the critical concentration limit c^* (*overlap concentration*) causes a change in the interactions to those characteristic of a semi-dilute system. The value of c^* (*overlap concentration*) is dependent on the biopolymer's molecular mass and represents average concentration of individual cluster segments. In the case of the lower the molecular mass, the higher the overlap concentration c^* means a lower concentration of chains, which when exceeded, results in diffusion (good solvent, **Figure 4B**) or aggregation (poor solvent, **Figure 4B**) of the molecules. Crossing the second overlap concentration c^{**} results in a formation of a concentrated solution, whose structure is close to a system of entanglements (good solvent) or phase separation is observed, which is caused by incompatibility (poor solvent). Conformation of the chain in a solution is dependent on the balance between osmotic pressure in the chain's close proximity (solvent absorption) and its elasticity, either enabling expansion or limiting it. The discussed behaviour is strongly related to temperature and the quality of the solvent, which is represented in **Figure 5**.

All the outlined consequences of the solvent-macromolecule and macromolecule-macromolecule interactions mean that the osmotic state equation should, as extensively as possible, take into account the interactions shaping the properties of a tested solution. Because of that, the applied virial state equation takes the following form:

$$\frac{\pi}{c_W} = \frac{RT}{M_n}\left[1 + A_2(T)c_W + A_3(T)c_W^2 + \ldots\right] \tag{1}$$

Its form is analogous to the virial equation of real gas. From a mathematical point of view, it can be considered as an expansion of the function into a series, around a solution corresponding to ideal solution behaviour. In that equation, $A_2(T)$ and $A_3(T)$ correspond to the second and third virial coefficients, c_W to biopolymer concentration, and M_n to the average osmotic molecular mass of the diluted substance. A detailed interpretation of Eq. (1) enables the analysis of the interactions between the diluted substance and the solvent and the molecules of the diluted substance. In the simplest interpretation, a negative value of $A_2(T)$ indicates a low affinity between a polymer and a solvent and in consequence, a probability of aggregation/association of the chains, or even precipitation or recrystallisation. High positive values of that coefficient, in turn, indicate a full compatibility of the solvent and the macromolecule.

4. Starch polysaccharides and osmotic properties of its pastes

Starch, which is produced and stored in plants seeds and bulbs, is one of the most important plant polysaccharides. It is composed of two types of biopolymers: amylose (AM) and amylopectin (AP). Amylose is a linear fraction composed of α-D-glucose units, bonded to each other through $\alpha(1 \rightarrow 4)$ glycosidic bonds, and its molecular mass is in the range from 100 to 1000 kg/mol (10^5–10^6 Da). Amylopectin has a higher molecular mass: 10^3–10^5 kg/mol (10^6–10^8 Da) and is heavily branched with $\alpha(1 \rightarrow 6)$ bonds [1–3]. There are only few known systems in which starch is soluble. They include water, dimethyl sulfoxide (DMSO) and N,N-dimethylacetamide with the addition of LiCl [4]. From the food industry perspective, the most important starch solvent is water. Dissolving starch requires a complete destruction of the starch granule, which is composed of layers of crystalline structure and amorphic layers [1–3]. The effect is a solution comprising both linear and branched chains. Their conformations and behaviour are different, and both are related to the type of solvent. Amylose, which in water solutions adopts a double helix conformation, starts to aggregate immediately after leaving the granule (precipitation combined with the formation of a crystalline structure, retrogradation [5] and after exceeding, overlap concentration (c^*) undergoes the gellation process [6, 7]. Amylopectin's conformation can be compared to a cluster with side chains sticking out. As a result, a structure is formed in which protruding chains of neighbouring macromolecules intersect and form an amorphic network of entanglements (**Figure 4**). The results of studies by Prof. Burchard's team seem to confirm above described phenomenon. (**Table 1**). A comparison of dimensions of $R_{g;branched}$ amylopectins with the $R_{g;linear}$ amyloses of the same molecular mass M_w:

$$g = \left(\frac{R_{g;branched}^2}{R_{g;linear}^2}\right)_{|M_w} \tag{2}$$

leads to a conclusion that AP chains exhibit smaller dimensions ($g < 1$) than amylose. The water solutions of amylopectin are stable and the chain intersections occur after exceeding the

Starch	AM, %	M_w, kg/mol	R_g, nm	A_2, 10^6 mol mL g^{-2}	c^*, g/L	g
Amylose*	100	150–750	25	–	–	–
Potato	24	51,000	222	8.96	7.9	0.166
Corn	22	88,000	213	3.65	3.1	0.077
Waxy corn	0	76,900	234	4.20	3.1	0.130
Amylstarch	76	16,700	231	3.14	17.0	0.168

The data concerns water starch solutions tested with the light scattering method SLS 20°C [2, 3]. M_w—weight average molecular mass, R_g—gyration radius, c^*—overlap concentration, A_2—second virial coefficient; all values were determined based on SLS measurements. *The results shown for amylose were carried out with chromatography methods.

Table 1. Molecular parameters of starch with varying amylose (AM) content.

overlap concentration c^* during a long period of time. If the concentration of AP in the solution is lower than c^*, then amylopectin clusters undergo a collapse [3] caused by the '*squeezing*' of water molecules.

For linear amylose, the interactions between its chains result in a formation of cluster structures (**Figure 4A**). Because of that, the molecular masses determined with the use of light scattering measurements (SLS) are significantly higher than those determined chromatographically for a single chain. The level of aggregation of AM chains depends on the initial concentration, at the start of dissolution. Dissolution of AM in water requires application of high temperatures of 135°C, as well as pressure. The authors of the Ref. [2] study carried out autoclaving at 10–15 bar. These distinct conformations of AM and AP raise a question about the nature of these chains' coexistence in water solutions: do amylose and amylopectin form separate structures and therefore are two separate components or whether they form a blend. Tests on solutions and pastes indicate the latter; however, phase separation is observed in those systems **(Figure 6)**.

Starch solutions obtained with the use of DMSO do not exhibit incompatibility with the solvent [8]. This behaviour is a result of the fact that the chains do not exhibit a tendency to aggregate. The values of the average radii of gyration and M_w obtained from SLS tests (**Table 2**) and chromatography are comparable [9]. A very small average radius of gyration obtained for the wax potato starch indicates a low level of branching of that amylopectin [10]. The test results presented in the Bello-Perez et al. [10] study indicate that both corn and potato amylopectins adopt spherical or globular conformation in DMSO. Amylose in DMSO adopts an
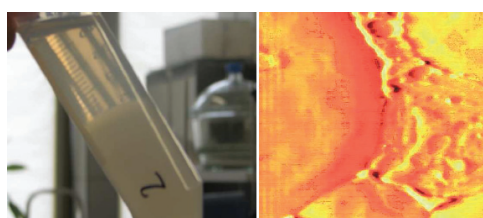

Figure 6. Incompatibility phenomenon in starch paste, AFM image of regular maize starch paste (right, own study, GONOTEC Qscope, USA, non-contact mode).

Starch	AM, %	M_w, kg/mol	R_g, nm	A_2, 10^3 mol mL g^{-2}
Amylose[1]	100	108–235	24–31	0.87–0.94
Potato[1]	24	26,000	127	0.0148
Waxy potato[2]	0	4000	15	–
Waxy corn[2]	0	53,000	242	–

The data concerns starch solutions in DMSO tested with light scattering method SLS at 20°C [7][1] and [8][2].

Table 2. Molecular parameters of starch with varying amylose (AM) content.

elastic chain conformation [8]. This finding is supported by the high values of the second virial coefficient (**Table 2**).

The mixture of DMSO and water can be used as a special solvent. These solutions exhibit a strongly non-ideal behaviour, due to the interactions between molecules. The methyl groups of DMSO may induce cooperative ordering in the system by hydrophobic hydration effects. The oxygen atom of a DMSO molecule can interact with water through H-bonding [10] with the continuum percolation transition in aqueous DMSO solutions with the percolation threshold of 12–15 wt.% of DMSO. A number of studies have been carried out over the years to understand the conformational properties of linear amylose [10–14] (**Table 3**) and branched amylopectin [14–17], in water and DMSO mixtures. The authors determined that the temperature and time of the dissolution have substantial influence on the weight average molecular mass, radius of gyration and the dispersion of the polysaccharide chains in the solution. With an increasing addition of water, the interactions between amylose and DMSO were reduced, leading to the conformational transition of AM from tight helical via loose helical to disordered coil [11]. The AP's solubility is limited by the presence of water in the solvent [17]. Increasing water content not only limits the AP's solubility but also causes an aggregation of its chains in

	Solution H$_2$O/DMSO	M_w, kg/mol	R_g, nm	A_2, 10^6 mol mL g^{-2}	α^2	Reference
	100/900	765	37.5	272	2.192	
AM	200/800	660	38.8	276	1.952	[16]
	500/500	555	34.0	123	1.304	
	700/300	506	26.3	55.6	1.189	
	100/900	151	84	–		[13]
	100/900	15,300	99.8			
	300/700	57,500	182.3			[19]
AP	500/500	192,700	182.8			
	100/900	171,000	238			[18]
	100/900	150,000	238	0.055		[13]

α^2—expansion coefficient.

Table 3. Molecular parameters of amylose and amylopectin in binary solvents H$_2$O/DMSO tested with light scattering method SLS at 25°C.

the solution. In the case of starch solutions in binary solvents, the phenomenon of coil overlap occurs.

In the case of utilising pure DMSO or DMSO/water mixtures, it is possible to achieve a decidedly higher solubility of starch and its derivatives than for pure water—up to 50% (w/w) starch solutions in pure DMSO [20] and in binary solvents ([21], the below photo from own studies).

For amylose solutions (**Figure 7**), a change in character of the π/c dependency can be observed: from ascending in the range of lowest concentration to descending for $c > 0.05$ g = 100 mL. The value of the second virial coefficient A_2 for the amylose solutions, determined based on the osmotic equation of state (EoS), is positive (**Table 4**). The third virial coefficient is negative, which indicates a possibility of aggregation or even recrystallisation of amylose in water solutions [6]. Additionally, this phenomenon is supported by the average osmotic molecular mass, whose value was estimated based on Eq. (1) to be 5500 kDa. The π/c relationships observed for AP and potato starch exhibit particularly interesting courses. In particular, it can be noted that the values of osmotic pressure are negative for certain concentrations of the polysaccharide. The negative values of π are related with the direction of flow of water in the measurement chamber of the device. The measurement of π consists of determining the pressure applied by the solvent, which flows to the measurement chamber through the membrane. When it comes to a negative signal, an opposite phenomenon is observed: a 'squeezing' of the solvent from the solution and its flow through the membrane into the chamber containing clear solvent. A phenomenon of water squeezing and collapse of the biopolymer coils was described in Ref. [2]. The critical concentration (*overlap concentration, c**), at which this phenomenon ceases, at
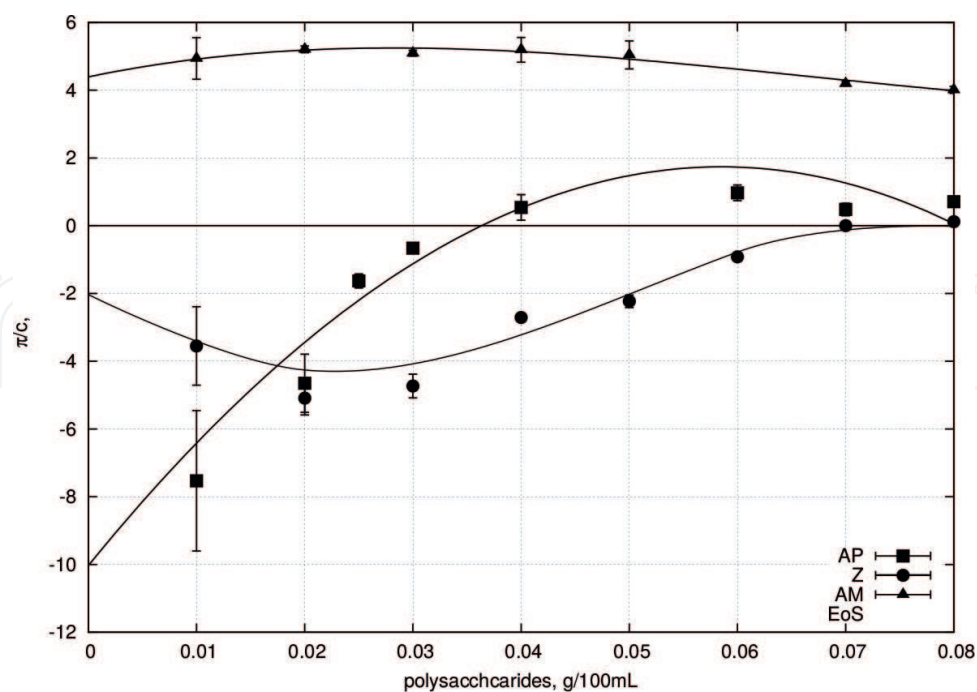

Figure 7. Correlation between reduced osmotic pressure π and concentration of water starch solutions (measurements carried out at 30°C using membrane osmometer GONOTEC Osmomat 090).

	Day	AM	AP	Starch native	Ac	Ph	E1404	M_w
30°C	1	$2.05 \cdot 10^{-6}$	$1.34 \cdot 10^{-5}$	$-1.09 \cdot 10^{-5}$	$4.17 \cdot 10^{-6}$	$1.06 \cdot 10^{-6}$	$-1.84 \cdot 10^{-6}$	$7.47 \cdot 10^{-7}$
	2		$4.42 \cdot 10^{-5}$	$4.17 \cdot 10^{-5}$				
	8		$4.17 \cdot 10^{-5}$	$4.48 \cdot 10^{-5}$				
40°C	1		$4.25 \cdot 10^{-5}$	$1.87 \cdot 10^{-5}$				
	2		$3.32 \cdot 10^{-5}$	$2.62 \cdot 10^{-5}$				
	8		$2.68 \cdot 10^{-5}$	$3.07 \cdot 10^{-5}$				

Table 4. Value of the second osmotic virial coefficient A_2 mol mL g^{-2} or native starches (amylose AM, amylopectin AP) and modified starches (acetylated Ac, starch phosphate Ph, starches oxidised with E1404 and oxidised with microwave radiation M_w).

25°C was: for AP 3.1 mg/mL (c* = 0.31 g/100 mL) and for potato starch 7.9 mg/mL (c* = 0.79 g/100 mL) [2, 3]. The concentrations observed on the charts, for which the π/c curve exceeds zero value, were 0.038 g/100 mL for AP and 0.074 g/100 mL for potato starch (at 30°C) and are therefore qualitatively consistent with the results of studies by Burchard and co-workers. This indicates that a concentration increase fosters the interactions between polysaccharide chains. Because of negative values of π, it was not possible to estimate the values of average osmotic molecular masses. Values of second and third virial coefficient were determined for amylopectin and potato starch pastes. At 30°C, the A_2 for AP measured $1.34 \cdot 10^{-5}$ mol mL g^{-2} and $A_3 < 0$. These results point to a high affinity of amylopectin to water (positive value of the second coefficient), with the ability to form local bundles of amylopectin clusters (negative third coefficient). These observations are consistent with literature results [20]. For the potato starch, the $A_2 = -1.09 \cdot 10^{-5}$ mol mL g^{-2} and $A_3 > 0$. These values indicate a gellation process caused by the presence of amylose.

4.1. The effect of time on osmotic properties of pastes

Storage of the pastes in room temperature causes changes in the interactions between their components (**Figure 8**). The results of osmotic pressure measurements at 30°C carried out 24 h after the first measurements (*day 2*) are similar to the behaviour of a fresh paste, however in the range of lower concentrations, a much lower osmotic pressure is observed. This probably indicates an increase of collapse of amylopectin chains. The overlap concentration for which the osmotic pressure becomes greater than zero has not changed. For *day-8* measurements, the osmotic pressure is not greater than zero in the analysed range of concentrations. The observed behaviours are the characteristic of dissolved solutions of amylopectin clusters, because they occur in the range of concentrations lower than overlap concentration, which for the reference temperature 25°C is the literature stated at 0.31 g/100 mL [2, 3]. However, positive values of A_2 (**Table 4**) indicate that water is a good solvent for amylopectin and are consistent with literature data. The measurements of osmotic pressure were also carried out at 40°C. The results are shown in **Figure 8**.

No qualitative changes in the course of the π/c curve were noted for the *fresh* solution compared to the relationship plotted at 30°C. Overlap concentration c* increases to the value of
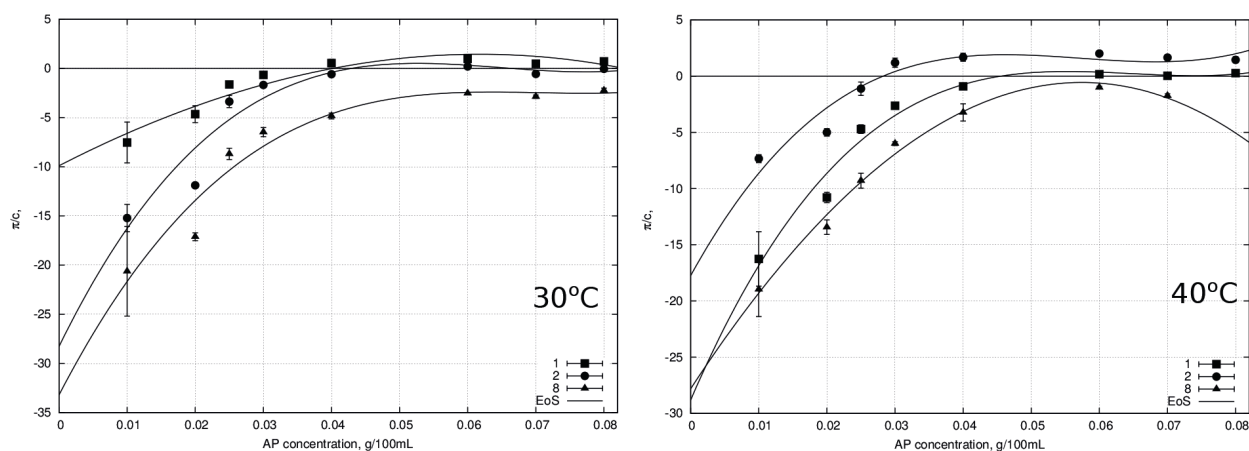
Figure 8. Correlation between reduced osmotic pressure π and water solution of amylopectin (AP) in the function of storage time of the solution (measurements carried out at 30 and 40°C using membrane osmometer GONOTEC Osmomat 090).

0.045 g/100 mL and the value of the second virial coefficient to $4.25 \cdot 10^{-5}$ mol mL g^{-2}. On the second day, the value of overlap concentration c^* decreases abruptly to 0.03 g/100 mL, which indicates an increase of *critical dimensions* of amylopectin clusters. The value of the second coefficient is still positive (**Table 4**), while $A_3 < 0$. After 8 days of storage, even an increase in measurement temperature does not result in significant qualitative or quantitative changes in the course of π/c in the function of concentration in comparison to the results of tests carried out at 30°C. Only the value of A_2 decreases slightly (**Table 4**), and the third virial coefficient is negative.

The measurements of π changes were also carried out for the potato starch pastes (**Figure 9**). On the second day of storage, a dramatic change in the interactions of solution's components was observed. After exceeding $c^* = 0.026$ g/100 mL, the osmotic pressure becomes positive. The course of the π/c curve points to two observations. Firstly, the critical radius of gyration of starch increases significantly, which is a result of a massive change in the overlap concentration in relation to the value obtained for *day 1*. This is related to the joint retrogradation of amylose
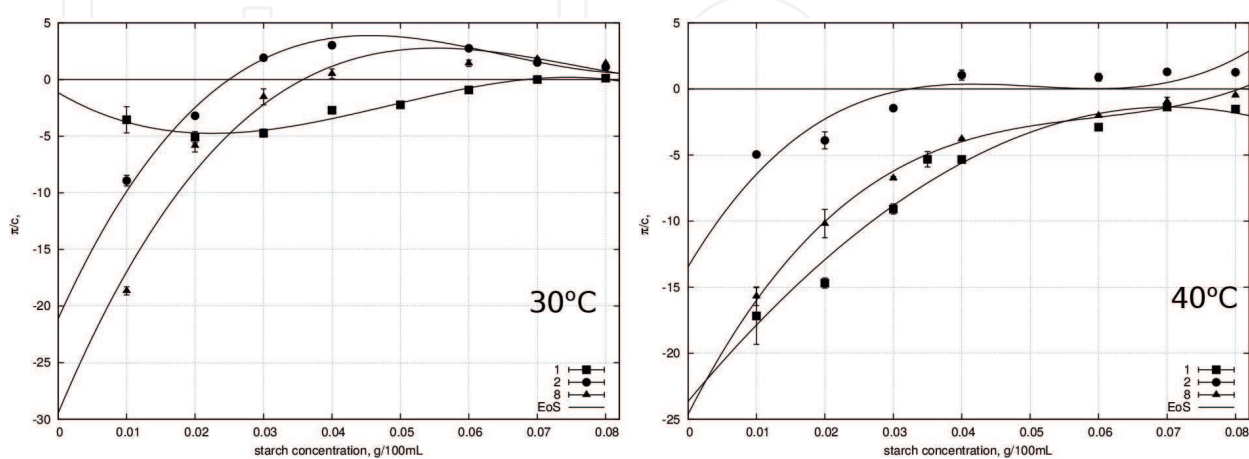

Figure 9. Correlation between the reduced osmotic pressure π and the concentration of water potato starch solution in the function of storage time (measurements carried out at 30 and 40°C, using a membrane GONOTEC Osmomat 090).

and amylopectin. Most probably, the presence of AP as a spatial hindrance accelerates the AM recrystallisation process. Secondly, an occurrence of behaviour characteristic of gelling systems is clearly observed because an increase of π/c value is noted followed by its decrease, similarly to the solutions of pure AM (**Figure 7**). The values of the second and third virial coefficients (**Table 4**) become positive. On *day 8* of storage, the value of the second virial coefficient is positive, while $A_3 < 0$. The value of c^* increases to 0.032 g/100 mL, which indicates a reduction of critical dimensions of chains present in the solution. Similar measurements carried out at 40°C indicate to structural changes at higher temperatures. The value of the second virial coefficient, determined based on measurement results carried out on the first day, is positive. However, the values of π are negative, and this is related to the *squeezing* of water from the clusters. In the discussed range of concentrations, the value of c^* cannot be determined. This could indicate a certain relaxation of the structure with an increase of distance between clusters. Properties of the mixture after 24 h of storage undergo changes. The values of π become positive for $c = 0.035$ g/100 mL, which indicates an increase of critical dimensions of the aggregates. On day 8, the occurrence of solvent *squeezing* is predominant (negative values of π) due to starch retrogradation.

Chemical modification of starch causes changes in the interactions between polysaccharide chains and water (**Figure 10**). For phosphorylated potato starch, the reduced osmotic pressure has negative values. This behaviour is different to the native potato starch, as for the tested range of concentrations (0.050–0.075 g/100 mL), the positive values of osmotic pressure were not observed. Based on that, it is possible to speculate that phosphorylation has caused the change to the overlap concentration, at which values of π would adopt positive values. This
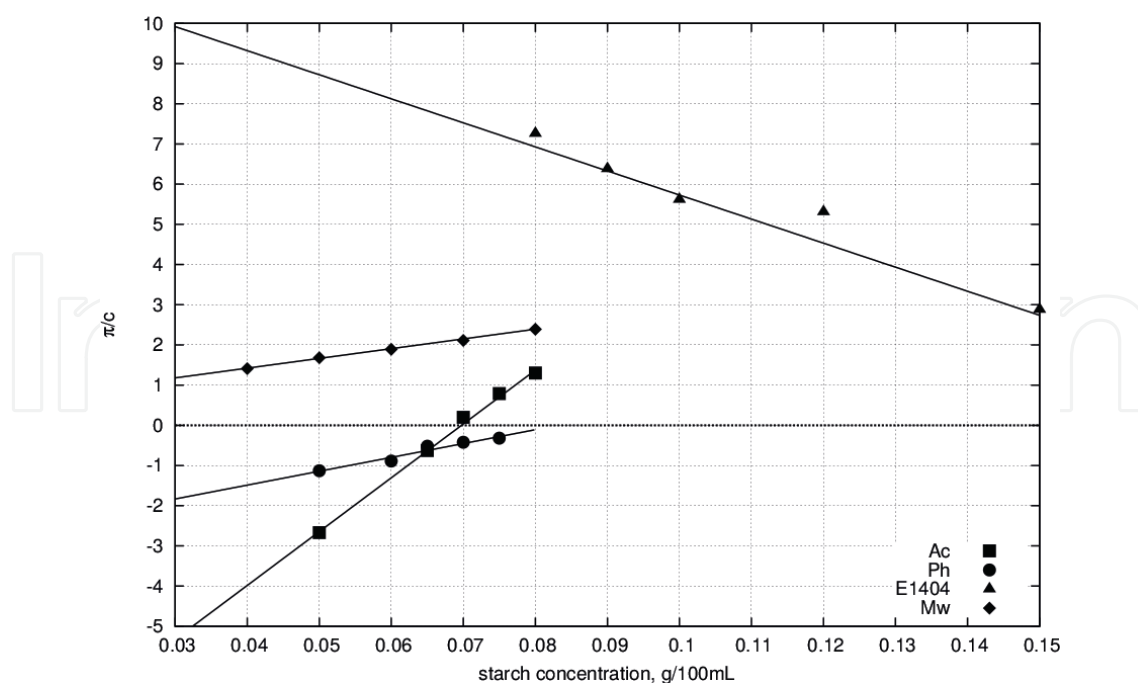

Figure 10. Correlation between reduced osmotic pressure π and concentration of water potato starch solutions: acetylated (Ac), phosphorylated (Ph), oxidised (E1404) and subjected to microwave radiation (M_w), in the function of concentration (measurements at 40°C).

implies, that in comparison to native potato starch, the chains of phosphorylated starch undergo contractions, also at higher concentrations of the solution. The second virial coefficient calculated for the obtained test data is positive, which indicates a change in the interactions between the solvent and polysaccharide. An increase in solvation of the biopolymer chains occurs.

Acetylation of starch, similarly to phosphorylation, causes a change to the concentration at which the values of osmotic pressure are positive. This results in a change of osmotic properties, which is in accordance to the results presented by Żmudziński et al. [22]. The values of reduced osmotic pressure are negative for concentrations in the range from 0.050 to 0.065 g/100 mL and positive from 0.070 to 0.080 g/100 mL. The correlation obtained for the tested systems is ascending for the whole range of concentrations. Positive values indicate an increase of water absorbability of the tested solutions. The second virial coefficient calculated for these systems has a positive value. An increase of the affinity of the solvent molecules to the polymer chains occurs, which means that water is a good solvent for acetylated starch.

For solutions of starch oxidised in a microwave radiation field, the obtained π/c values are positive in the whole range of concentrations. The obtained π/c correlation is ascending. This behaviour indicates that this starch modification in these particular conditions causes an increase in water absorption by the potato starch chains, which can be related to an easier access of solvent to the starch granules. The determined virial coefficient is positive, which allows us to deduce an improvement of permeability and solvation of starch chains due to the microwave radiation.

The values of the reduced osmotic pressure obtained for the oxidised starch (E1404) are the highest of all tested systems; however, the obtained correlation is descending. It is worth noting that the concentration range included higher concentrations than for the other systems. A common concentration for the tested starches is 0.080 g/100 mL, for which the value of π/c is approximately seven times higher than for the acetylated starch and approximately four times higher than for the starch treated with microwaves. The obtained results indicate to the absorption of water by the starch chains. The second virial coefficient is negative but higher than for native starch, which indicates approximately 10 times more dissolution capability than native potato starch.

5. Non-starch polysaccharides

The non-starch polysaccharides group includes gums of various plant origin: locust bean gum, konjac, guar gum and carrageenans or bacterial origin polysaccharide: xanthan and chemical modified cellulose: carboxylmethylcellulose.

Locust bean gum (carob gum) is obtained by the milling of endosperm of the seeds from the carob tree pods (*Ceratonia siliqua L.*, belonging to *Fabaceae* family), vegetation characteristic for the Mediterranean regions. The endosperm in the seeds takes approximately 42–46%, the remaining parts are bran husk 30–33% and germ 23–25% [23]. The extraction of carob gum can be carried out by two methods. The first comprises thermo-mechanical or chemical

separation of the bran husk, and then separation of the germ from the endosperm and finally subjecting the endosperm to milling, sieving and sorting. The second method uses a combination of extraction and purification [24, 25]. Whole brans are subjected to milling and then extracted using water and precipitation with the use of alcohol (ethanol or isopropanol) [26–28]. The flour is a non-ionic biopolymer belonging to galactomannans; therefore, the main chain of this polysaccharide is formed by mannose units joined by β-(1,4)-glycosidic linkages, to which single units of D-galactopyranose are attached by the α-(1,6) linkages. In the carob gum, the side branches are not positioned symmetrically; therefore, unsubstituted β-D-mannopyranose units can occur [29, 30]. The ratio of mannose to glucose ranges between 3.1 and 3.9 [31–33] and depends on the variety, source and most of all on the applied extraction method [33]. The galactose content of approximately 20% is lower in comparison to other galactomannans, such as guar gum and tara gum [28, 34]. The ratio of mannose to galactose (M/G) has impact on this polysaccharides solubility in water [31, 35], the higher ratio of (M/G) results in better thickening properties [35]. Side chains in the form of attached mannose units at the C-6 carbon position contain arabinose residues [31]. Galactomannans exhibit a polymer structure of '*random coils*'; therefore, high temperature and energetic mixing are required for their complete dissolution in water (to achieve best water binding) [34, 37]. The locust bean gum was the first to be used not only in food industry but also in the production of textiles, paper, pharmaceuticals and cosmetics [36, 38].

Guar gum is a non-ionic polysaccharide obtained from the endosperm of guar seeds (*Cyamopsis tetragonoloba*, from the family *Leguminosae*). The extraction methods are similar to those used for extraction of the locust bean gum and comprise separation of shells, milling and extraction [34, 39], sometimes enzymatic processing or extrusion is also utilised. The main chain of this polysaccharide is formed by D-mannose units linked by β-(1,4)-glycosidic linkages and also contains single units of D-galactose, attached to the main chain by the α-(1,6)-glycosidic linkages. The ratio of mannose to glucose is approximately between 1.5:1 and 1.8:1 [29, 40] or approximately 2:1 [36]. The ratio of mannose to glucose together with the molar mass of this polysaccharide depends on the variety of the seed from which it is extracted and affects its solubility, thermal stability and rheological properties [38, 41]. Guar gum is widely used in the food, cosmetic and mining industries [43–45].

Konjac gum is obtained from the tubers of the *Amorphophallus konjac* plant, belonging to the *Araceae* family and farmed in Asia. The tubers of the konjac plant grow and enlarge throughout the plants lifetime. Among the products obtained from konjac tubers, depending on the purification degree, are: konjac flour, konjac gum and purified konjac glucomannan. Two-year-old tubers are used for the production of konjac flour, as after 3–5 years they bloom and are used as seed material. The content of konjac glucomannan in the bulbs ranges from 8 to 10%, and the remaining components are starch, proteins, fats and mineral components [43, 46]. The main component of konjac gum is the konjac glucomannan, a neutral heteropolysaccharide formed by D-mannose and D-glucose, joined by β-(1,4)-glycosidic linkages. Molar ratio of mannose to glucose is 1.6:1 [47–50]. The main chain is slightly branched by glucose units in the C-6 carbon position [51, 52]. The branching can also occur in the C-3 carbon position, both for mannose and glucose [42]. The degree of branching of the polysaccharide chain is approximately 8%. Moreover, native glucomannan exhibits a slight degree

of acetylation (DS) from 0.05 to 0.1 (1 in 12 or 18 sugar units) [51, 53, 54]. The chain acetylation affects its solubility. Konjac gum is soluble in water and, due to high possibilities of water binding, forms solutions of high viscosity [50, 55]. Similarly to other hydrocolloids, such as xanthan gum or carrageenan, it forms gels [56, 57]. It is widely used in food, pharmaceutical and cosmetic industries [51, 58].

Gum arabic is a natural plant sap excretion harvested from acacia trees (*Acacia Senegal* and *Acacia seyal*) [59–60] and is obtained by cutting holes into the bark. The sticky sap dries on the trees, forming hard lumps, which are collected and sorted and then grounded. Another production method comprises the dissolution of gum arabic in water at low temperatures, so that its denaturation would not occur, and then, the obtained solution is subjected to decantation or filtration. Afterwards, it is subjected to pasteurisation and in the last stage, the mixture is subjected to drying [53, 61]. The structure of the gum arabic is rather complex. The main chain of this polysaccharide is formed by (1,3) and (1,6) β-D galactopyranose units, connected with (1,6) β-D-glucopyranose units of uronic acid. The side chains can contain units of α-L-ramnopyranose, β-D-glucuronic acid, β-D-galactopyranose units and α-L-arabinofuranose units [59, 62–64]. The main characteristic of gum arabic is its covalent bond with the protein chain [59]. It is known that a protein molecule rich in hydroxyproline (Hyp), serine (Ser) and proline (Pro) constitutes the core, to which polysaccharide units connect via Ara-Hyp (Ara—arabinose) linkages. The polysaccharide chains coil into globular units and '*decorate*' the protein chain in such a way as to achieve an overall spheroidal shape [59, 66]. Gum arabic is highly soluble in water (up to 50% w/v), and its solutions have relatively low viscosity in comparison to other plant gums. This is a result of the highly branched molecular structure and relatively low molecular mass of this polymer [54]. The protein part of the gum arabic is responsible for the surface activity and has impact on the foam forming and emulsifying properties of this polymer [63, 67, 68]. Currently, it is used as a food additive, a component in pharmaceutical industry and is also utilised for technical purposes [64, 69].

Xanthan gum is an extra-cellular polysaccharide produced by the *Xanthomonas campestris* bacteria on the cell wall surface during a complex enzymatic process [70, 71]. On the industrial scale, xanthan gum is produced with the use of pure bacteria cultures in a submerged aerobic fermentation process. The bacteria cultivation happens in an adequately aerated environment containing glucose, nitrogen sources and other trace elements. In order to ensure an adequate efficiency, the fermentation process is divided in several stages. After the last stage of fermentation, the obtained bullion is pasteurised and the xanthan gum is extracted by precipitation with isopropyl alcohol. The final stages of production include drying and grinding [54]. The basic structure of xanthan gum includes cellulose skeleton formed of β-(1,4) D-glucose units, substituted alternatively by glucose with trisaccharide chain units at C-3 carbon position. This chain is formed by two mannose units, separated by (D)-glucuronic acid. The acid is attached to the external (D)-mannose unit by a β-(1,4) linkage, and to the internal one by the β-(1,2) glycosidic bond, which in turn is bound to the glucose of the main chain by a β-(3,1)glycosidic linkage [72, 73]. Approximately half of the end mannose units at C-6 carbon have an attached purine group, while the internal units at C-6 carbon position have acetyl groups attached. Xanthan gum is therefore a pentamer, and each molecule contains approximately 7000 of them [65]. The chain of xanthan gum may also have a structure of single or triple helix [66]. It is soluble in cold

water forming solutions of high apparent viscosity (i.e., 1% solution 1.2–1.6 Pa·s). Solutions of xanthan gum are pseudo-plastic liquids, this is a result of the molecules ability to form aggregates by hydrogen bonds and polymer entanglements. Thanks to that, a pseudogel structure is formed, allowing practical uses of xanthan gum solutions [54].

Carboxymethylcellulose (CMC) is a half-synthetic anionic polysaccharide obtained by chemical modification of cellulose. During the process, a partial substitution by carboxymethyl group occurs of the second, third and sixth hydroxyl groups in cellulose. The linear chains of CMC are formed of glucose units joined by β-(1,4)glycosidic linkage. Average substitution CMC level is defined as an average number of carboxymethyl groups repeating unit. This parameter is defined in the range 0.4–1.5. This polymer is usually available in the form of sodium salt, and the product soluble in water is characterised by the substitution level above 0.5. Molar mass of this polymer is varied, for example, it can be in the range $2.5 \cdot 10^{-5}$–$7.0 \cdot 10^{-5}$ g mol^{-1}. CMC is widely used in the food, cosmetic, paper, textile and drilling industries [76, 77].

Carrageenans are a group of polysaccharides, in which 15 types can be distinguished, differing between each other based on structure. These polysaccharides are obtained by alkaline extraction of red edible seaweeds. The ι-, κ-, λ-carrageenan are mainly used in practical application. The main native polysaccharide chain of these three fractions is formed by a repeated poly-(1,3)-[4-sulphate-β-D-galactopyranose-(1,4)-3,6-anhydro-2-sulphate-α-D-galactopyranose]. κ-Carrageenan poly-(1,3)-[4-sulphate-β-D-galactopyranose-(1,4)-3,6-anhydro-α-D-galactopyranose]. λ-Carrageenan poly-(1,3)-[2-sulphate-β-D-galactopyranose-(1,4)-2,6-anhydro-α-D-galactopyranose]. κ- and ι-Carrageenans, as opposed to the lambda fraction, form thermo-reversible gels. Above the melting temperature, the chains of this polymer occur in the form of coils, and during the lowering of temperature, the coils change the conformation to double helices and form larger aggregates and thus form a spatial gel network structure [78, 79].

5.1. Osmotic properties of nonstarch polysaccharides' solutions

The tests on the osmotic properties of the polysaccharides water solutions were carried out using a membrane osmometer at two temperatures: 30 and 40°C. For the solutions of locust bean gum (LbG), the relation of the reduced osmotic pressure (π/c) to the concentration (c) at both temperatures was descending in the whole range of tested concentrations. It was observed, that after exceeding c^* (1.5), the values of π/c undergo little changes (for the three highest concentrations). In that range of concentrations, higher values of π/c were noted at temperature of 40°C, which could be explained by the fact that increased temperature causes lower aggregation of biopolymer chains than the 30°C temperature. This interpretation of the phenomenon is also influenced by the interactions of biopolymer-biopolymer type. Below c^*, two concentrations can be distinguished, at which a change in the behaviour of the tested solutions occurs. Namely, for the concentration of 0.1 g/100 mL, the reduced osmotic pressure assumes a higher value at 40°C. The reversal takes place at the concentration of 1.5 g/100 mL, and a return to higher values of π/c at 40°C was observed for the concentration of 0.4 g/100 mL>c^*. The values of the second virial coefficient determined for both temperatures are negative (**Table 5**). This indicates to a low affinity of the solvent to the polysaccharide chains. An increase of measurement temperature from 30 to 40°C causes a small change of the value of this

	M_w, g mol^{-1}	c^*, g dL^{-1}	Reference	30°C	40°C	M_w^{osm}, g mol^{-1}
KG	10^5–10^6	0.08	[87, 89]	$-2.52 \cdot 10^{-6}$	$-8.14 \cdot 10^{-7}$	$0.24 \cdot 10^5$
GG	$9.1 \cdot 10^5$	0.13				
	$7.3 \cdot 10^5$	0.28		$-2.43 \cdot 10^{-7}$	$-5.40 \cdot 10^{-7}$	$1.6 \cdot 10^5$
	$4.0 \cdot 10^5$	0.45	[70]			
	$2.7 \cdot 10^5$	0.45				
LbG	$0.697 \cdot 10^6$–$0.94 \cdot 10^6$	0.4	[71]	$-2.02 \cdot 10^{-7}$	$-2.20 \cdot 10^{-7}$	$1.4 \cdot 10^5$
	$1.94 \cdot 10^6$–$2.29 \cdot 10^6$	0.33	[72]			
XG		0.03	[72, 84]	$-1.36 \cdot 10^{-4}$	$-8.02 \cdot 10^{-5}$	
CMC	$3.5 \cdot 10^4$–$1.7 \cdot 10^6$	–	[68]	$-9.84 \cdot 10^{-5}$	$-1.58 \cdot 10^{-4}$	$2.57 \cdot 10^6$
AG	$5 \cdot 10^5$–$6.5 \cdot 10^5$	–	[74]	$2.80 \cdot 10^{-7}$		$1.07 \cdot 10^6$
CA	$6.6 \cdot 10^3$–$1.2 \cdot 10^6$	–	[75]	$-8.41 \cdot 10^{-6}$		$0.08 \cdot 10^5$

Table 5. Average molecular masses, values of the first overlap concentration and values of the second osmotic virial coefficient A_2 mol mL g^{-2} for:

coefficient, which suggests that in that range of temperatures, only a small increase of solubility of LbG chains in water takes place (**Figure 11**).

In the case of guar gum solutions (GG), the measurements were done in the same range of concentrations as for LbG, both $<c^*$ as well as $>c^*$. The value (c^*) is confirmed by the study by Baines and Morris [76]. The values of reduced osmotic pressure exhibit a decreasing tendency with an increase of polysaccharide concentration. Initially (concentration range 0.1–0.3 g/100 mL), the reduced osmotic pressure assumes higher values at 30°C temperature. The reversal of this behaviour occurs only at the 0.4 g/100 mL concentration. In the final range of concentrations (0.45–0.5 g/100 mL), the highest values of π/c were noted at 30°C temperature, which indicates a different behaviour than in the case of LbG. Exceeding c^* results in an increase of the degree of chain aggregation and an increase of influence of biopolymer-biopolymer interactions, the effects of which are more visible at 40°C temperature. The second virial coefficient assumes
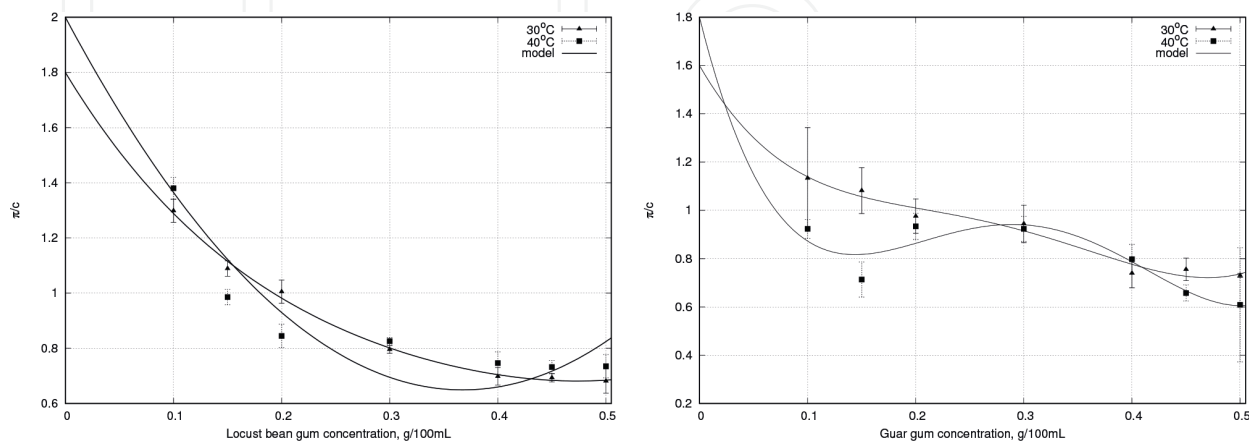

Figure 11. Correlation of reduced osmotic pressure π and the concentration of water solutions of locust bean gum and guar gum in the function of concentration (measurements at 30 and 40°C).

negative values for both temperatures [80–83]. At 40°C, a two times lower value was noted for this polysaccharide, than at 30°C, which can be interpreted as a decrease of the tendency of GG chains to solvation. An increase in temperature, therefore, causes an increase in solubility. Exceeding c^* (in our case 0.3 g/100 mL) causes the values of π/c at 40°C temperature to be similar to those obtained at 30°C. At concentration of 0.4 g/100 mL, the value of π/c is visibly higher at 40°C than at 30°C. This could be explained by the fact that for a certain range of concentrations, after exceeding c^*, an increase of temperature causes the infiltration of solvent particles into the chains. However, above the concentration of 0.4 g/100 mL, due to an increasing force of biopolymer-biopolymer interactions, a decrease of the π/c value is observed. Both for GG and LbG, we are looking at a 'random coil' chain structure, which impedes the penetration of the solvent into the polysaccharide chain. Low values of π/c (0.6–1.4 mmH$_2$O/g dL^{-1}) for both gums indicate low water absorption of these polysaccharides in the studied range of concentrations (**Figure 12**).

Xanthan gum solutions (XG) were tested in the range of concentrations below c^* (**Table 5**). The relation of the reduced osmotic pressure and the concentration at 40°C temperature, as for the above described cases, is descending (**Figure 13**). At 30°C temperature, two areas are observed: of decreasing and increasing π/c. Higher values were noted for the 40°C temperature, which could be explained by a change of the polymer chain conformation from helix to coil. Helical structures exhibit high rigidity which hinders the movement of the solvent in the solution. This behaviour changes due to increased temperature and the helix-coil transformation. The noted values of π/c were contained in the range from 10 to 40 mmH$_2$O/g dL^{-1}. The virial coefficients, as for all the other cases, are negative. At 40°C, the value of A_2 is 10 times higher than at 30°C, which confirms the influence of temperature on the Xanthan gum chain solvation interactions.

The correlation of π/c and concentration obtained for the konjac gum is descending at both temperatures. The tests were carried out at concentrations below c^* (**Table 5**). The values of π/c obtained at 40°C temperature are approximately two times lower than at 30°C. This indicates that an increase of temperature does not increase the affinity of konjac gum chains to the
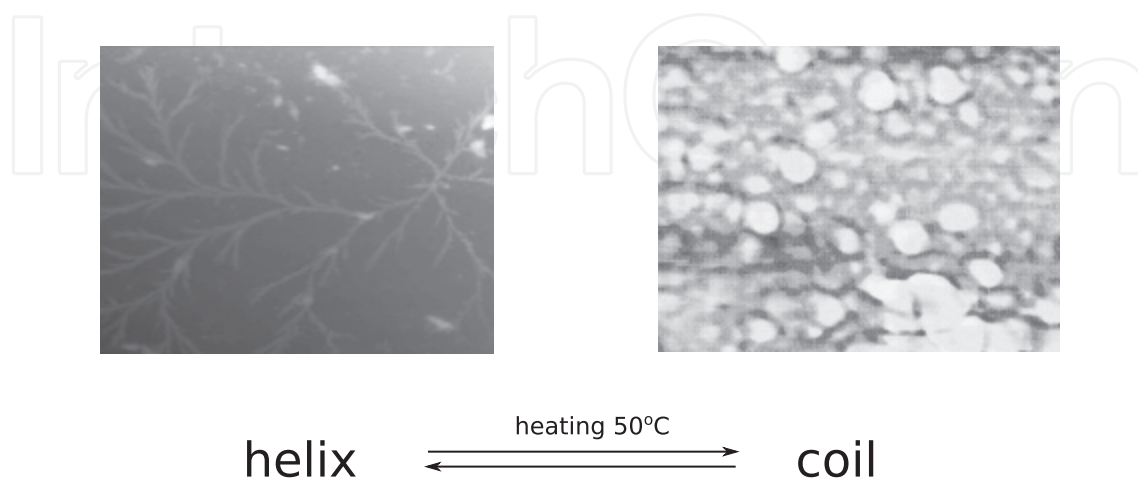

helix $\rightleftarrows$ coil

heating 50°C

Figure 12. Structure changes of xanthan gum chains in water solutions, AFM images (own study, GONOTEC Qscope, USA, non-contact mode).
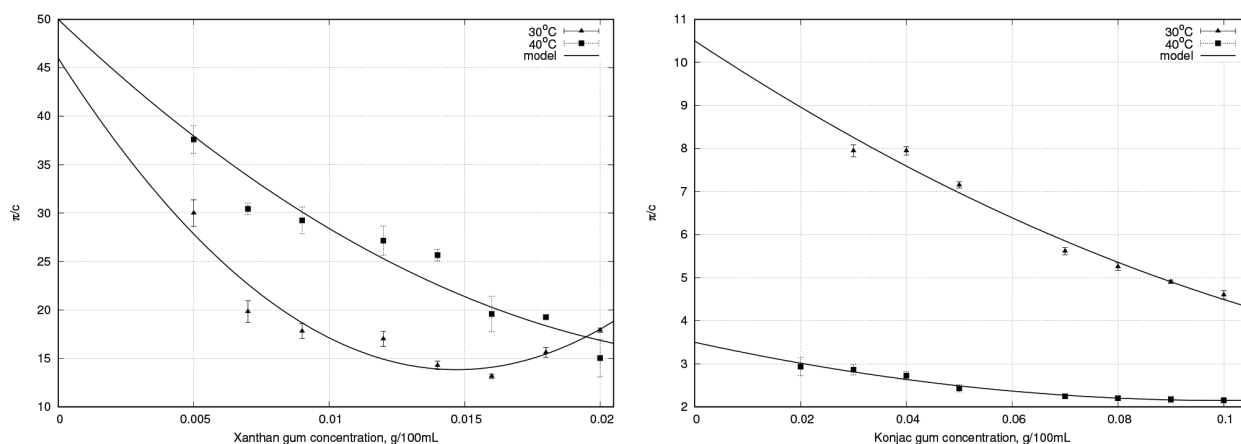
Figure 13. Correlation of the reduced osmotic pressure π and the concentration of xanthan gum (left) and konjac (right) water solutions in the function of concentration (measurements at 30 and 40°C).

solvent. This situation can be due to high viscosity of this polysaccharides solutions (viscosity effect), which hinders the movement of solvent in the solution and by the presence of protein in the konjac gum preparations, which can hinder contact between the solvent and the polysaccharide. Moreover, such behaviour can be a result of this polysaccharides tendency to gelling. Negative virial coefficient confirms low affinity of polymer chains to the solvent.

In the case of carboxymethylcellulose (CMC) (**Table 5**) significantly different behaviours are observed, than in the above-mentioned examples, as the obtained correlation is ascending in the whole range of concentrations (0.005–0.02 g/100 mL) and temperatures (**Figure 14**). Slow increase of the reduced osmotic pressure is a result of high viscosity of the solution, which hinders the migration of the solvent in the solution. High values of π/c (up to 250 mm H_2O/g dL^{-1}) indicate that the CMC chains have the ability to absorb water. This is closely related to the CMC chains conformation in water, where they are completely straight. Such system results in the highest hydrodynamic radius and facilitation of solvation. An increase
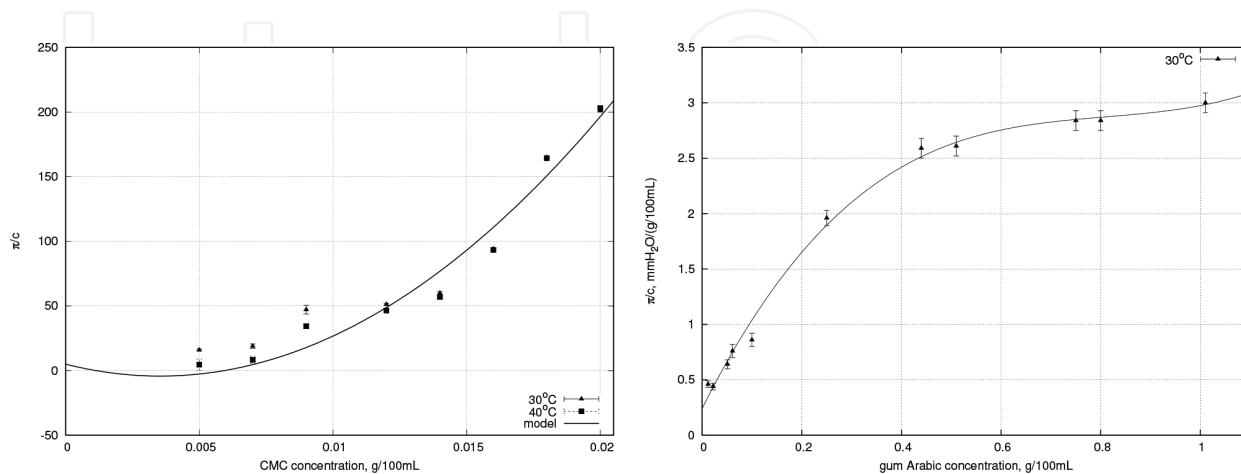

Figure 14. Correlation of the reduced osmotic pressure π and the concentration of carboxylmethylcelullose (left) and gum arabic (right) water solutions in the function of concentration (measurements at 30 and 40°C).

of temperature causes slight changes in the value of π/c reduced osmotic pressure. The second virial coefficient at the tested temperatures is negative and assumes the same value for both 30 and 40°C, which confirms the lack of influence of temperature on the osmotic properties of the studied CMC solutions. It should be noted that the value of the second virial coefficient is the lowest among all the tested hydrocolloids, where its value was negative; this is due to the viscosity effect.

For gum arabic, the relation of π/c to the concentration is ascending (**Figure 14**), similarly to the CMC solutions. However, an increase of gum arabic causes a much faster increase of the π/c value than for the CMC solutions. These observations are closely related to the structure of the gum arabic chain, which is formed of a protein chain with attached polysaccharide chains. Such structure results in a large contact area of polysaccharide chains and the solvent. More-over, the low viscosity, compared to CMC solutions, does not prevent migration of the solvent in the solution. The calculated value of the second virial coefficient is positive, which enables us to assume, that strong interactions occur between the biopolymer and the solvent and therefore, water is a good solvent for this type of systems [85, 86].

The π/c correlation obtained for carrageenan water solutions is descending in the whole range of concentrations (**Figure 15**). From the concentration of 0.25 g/100 mL, the decrease of the π/c value is less dramatic than for lower concentrations [88]. A negative second virial coefficient would suggest a low affinity of the solvent to the polymer chains, which is due to the low temperature of the osmotic pressure measurement.
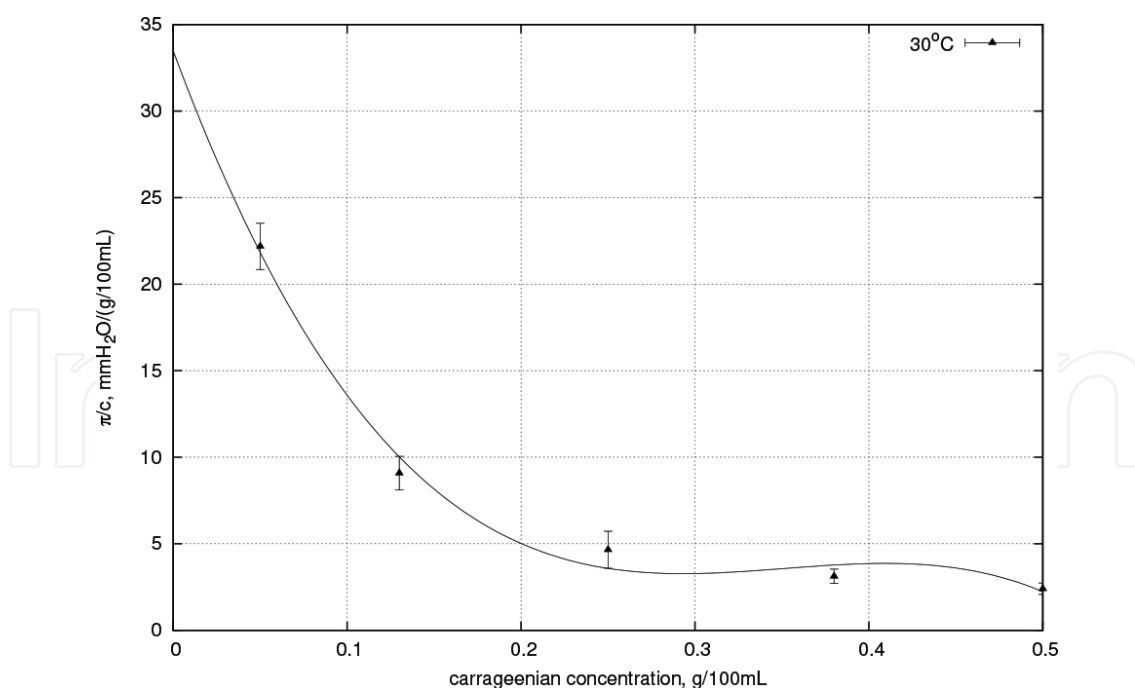

Figure 15. Correlation of the reduced osmotic pressure π and the concentration of carrageenan water solutions in the function of concentration (measurements at 30°C).

Author details

Kruk Joanna, Pancerz Michał and Ptaszek Anna*

*Address all correspondence to: a.ptaszek@ur.krakow.pl

Department of Engineering and Machinery for Food Industry, Faculty of Food Technology,
Agriculture University in Krakow, Kraków, Poland

References

[1] Eliasson A-C, editor. Starch in Food: Structure, Function and Applications. Cambrigde: Woodhead Publishing Limited; 2004

[2] Aberle T, Burchard W, Vorwerg W, Radosta S. Conformational contributions of amylose and amylopectin to the structural properties of starches from various sources. Starke. 1994;**46**:329-335. DOI: 10.1002/star.19940460903

[3] Aberle T, Burchard W. Starches in semidilute aqueous solution. Starke. 1997;**49**:215-224. DOI: 10.1002/star.19970490602

[4] Ghosh S, Chattoraj S, Chowdhury R, Bhattacharyya K. Structure and dynamics of lyzozyme in DMSO-water binary mixture: Fluorescence correlation spectroscopy. RSC Advances 2014;**4**:14378-14384. DOI:10.1039/C4RA00719K

[5] Heineck ME, Cardoso MB, Giacomelli FG, da Silveira NP. Evidences of amylose coil-to-helix transition in stored dilute solutions. Polymer. 2008;**49**:4386-4392. DOI: 10.1016/j.polymer.2008.07.062

[6] Miles MJ, Morris VJ, Orford PD, Ring SG. The roles of amylose and amylopectin in the gelation and retrogradation of starch. Carbohydrate Research. 1985;**135**:271-281. DOI: 10.1016/S0008-6215(00)90778-X

[7] Tester RF, Morrison WR, Swelling and gelatinization of cereal starches. I. Effects of amylopectin, amylose and lipids. Cereal Chem. 1990;**67**:551-557

[8] Radosta S, Haberer M, Vorwerg W. Molecular characteristics of amylose and starch in dimethyl sulfooxide. Biomacromolecules. 2001;**2**:970-978. DOI: 10.1021/bm0100662

[9] Ring SG, L'Anson KJ, Morris VJ. Static and dynamic light scattering studies of amylose solutions. Macromolecules. 1985;**18**:182-188. DOI: 10.1021/ma00144a013

[10] Bello-Perez LA, Roger P, Baud B, Colonna P. Macromolecular features of starches determined by aqueous high-performance. Size exclusion chromatography. Journal of Cereal Science. 1998;**27**(3):267. DOI: 10.1094/CCHEM.1998.75.4.395

[11] Roy S, Banerjee S, Biyani N, Jana B, Bagchi B. Theoretical and computational analysis of static and dynamic anomalies in water-DMSO binary mixture at low DMSO concentration. J. Phys. Chem. B. 2011;**115**:685-692. DOI: 10.1021/jp109622h PMID: 21186810

[12] Jordan RC, Brant DA. Unperturbed dimensions of amylase in binary water/dimethyl sulfoxide mixtures. Macromolecules. 1980;**13**:491-499. DOI:10.1021/ma60075a006

[13] Cheetham NWH, Tao L. Amylose conformational transitions in binary DMSO/water mixtures. Carbo-hydr. Polym. 1998;**35**:287-295. DOI: 10.1016/S0144-8617(97)00151-3

[14] Divers T, Balnois E, Feller JF, Spevacek J, Grohens Y. The influence of O-formylation on the scale of starch macromolecules association in DMSO and water. Carbohydr. Polym. 2007;**68**:136-145. DOI: 10.1016/j.carbpol.2006.07.026

[15] De Vasconcelos CL, de Azevedo FG, Pereira MR, Fonseca JLC. Viscosity-temperature-concen-tration relationship for starch-DMSO-water solutions. Carbohydr. Polym. 2000;**41**:181-184. DOI: 10.1016/S0144-8617(99)00078-8

[16] Han JA, Lim ST. Structural changes of corn starches by heating and stirring in DMSO measured by SEC-MALLS-RI system. Carbohydr. Polym. 2004;**55**:265-272. DOI: 10.1016/j.carbpol.2003.09.00

[17] Chakraborty S, Sahoo B, Teraoka I, Gross RA. Solution properties of starch nanoparticles in water and DMSO as studied by dynamic light scattering. Carbohydr. Polym. 2005;**60**:475-481. DOI: 10.1016/j.carbpol.2005.03.011

[18] Yang C, Meng B, Chen M, Liu X, Hua Y, Ni Z. Laser-light-scattering study of structure and dynamics of waxy corn amylopectin in dilute aqueous solution. Carbohydrate Polymers. 2006;**64**:190-196. DOI: 10.1016/j.carbpol.2005.11.017

[19] Ptaszek P, Lukasiewicz M, Ptaszek A, Grzesik M. Rheological scaling properties of starch solutions in dimethylsulfoxide. Chemical and Process Engineering. 2012;**33**:323-333. DOI: 10.2478/v10176-012-0029-7

[20] Ptaszek P, Lukasiewicz M, Ptaszek A, Grzesik M. Rheological scaling properties of starch solu-tions in dimethylsulfoxide. Chemical and Process Engineering. 2012;**33**:323-333. DOI: 10.2478/v10176-012-0029-7

[21] Ptaszek A, Ptaszek P, Dziubiński M, Grzesik N M, Liszka-Skoczylas M. The effect of structural properties on rheological behaviour of starches in binary dimethyl sulfoxide-water solutions. Plos One. 2017;**2**:1-15. DOI:10.1371/journal.pone.0171109

[22] Żmudziński D, Ptaszek A, Grzesik M, Kruk J, Kaczmarczyk K, Liszka-Skoczylas M. Influence of starch acetylation on selected rheological properties of pastes. Starch-Starke. 2014;**66**:303-315. DOI: 10.1002/star.201300094

[23] Dakia PA, Blecker C, Robert C, Wathelet B, Paquot M. Composition and physicochemical properties of locust bean gum extracted from whole seeds by acid or water dehulling pre-treatment. Food Hydrocolloids. 2008;**22**:807-818. DOI: 10.1016/j.foodhyd.2007.03.007

[24] Ensminger AH, Ensminger ME, Konlande JE, Robson JRK. Food and Nutrition Encyclo-pedia. 2nd ed. Vol. 1. Boca Raton: CRC Press LLC; 1994. pp. 346-348

[25] Daas PJH, Schols HA, de Jongh HHJ. On the galactosyl distribution of commercial galactomannans. Carbohydrate Research. 2000;**329**:609-619. DOI:10.1016/S0008-6215(00)00209-3

[26] McCleary BV, Matheson NK. α-D-galactosidase activity and galactomannan and galacto-syl-sucrose oligosaccharide depletion in germinating legume seeds. Phyfochemistry. 1974;**13**:1747-1757. DOI: 10.1016/0031-9422(74)85084-3

[27] da Silva IAL, Gomçalves MP. Studies on a purification method for locust bean gum by precipita-tion with isopropanol. Food Hydrocolloids. 1990;**4**(4):277-287. DOI: 10.1016/S0268-005X(09)80204-X

[28] Lazaridou A, Biliaderis CG, Izydorczyk MS. Structural characteristics and rheological proper-ties of locust bean galactomannans: a comparison of samples from different carobtree populations. J Sci Food Agric. 2000;**81**:68-75. DOI: 10.1002/1097-0010(20010101)81:13.0.CO;2-G

[29] Dea ICM, Morrison A. Chemistry and interactions of seed galactomannans. Adv. Curbohydr. Chem. Biochem. 1975;**31**:241-312. DOI: 10.1016/S0065-2318(08)60298-X

[30] Daas PJH, Schols HA, de Jongh HHJ. On the galactosyl distribution of commercial galac-tomannans. Carbohydrate Research. 2000;**329**:609-619. DOI:10.1016/S0008-6215(00)00209-3

[31] Gainsford SE, Harding SE, Mitchell JR, Bradley TD. A comparison between the hot and cold water-soluble fractions of two locust bean gum samples. Carbohydrate Polymers. 1986;**6**:423-442. DOI: 10.1016/0144-8617(86)90002-0

[32] McClary BV.The fine structures of carob and guar galactomannans. Carbohydrate Research. 1985;**139**:237-260. DOI: 10.1016/0008-6215(85)90024-2

[33] Körk MS. A comparative study on the compositions of crude and refined locust bean gum: In re-lation to rheological properties. Carbohydrate Polymers. 2007;**70**(1):68–76. DOI:10.1016/j.carbpol.2007.03.003

[34] Richardson PH, Willmer J, Foster TJ. Dilute solution properties of guar and locust bean gum in sucrose solutions. Food Hydrocolloids. 1998;**12**:339-348. DOI: 10.1016/S0268-005X(98)00025-3

[35] Körk MS, Hill SE, Mitchel JR. A comparison of the rheological behaviour of crude and refined locust bean gum preparations during thermal processing Carbohydrate Polymers 1999;**38**(3):261-265. DOI:10.1016/S0144-8617(98)00100-3

[36] Simões J, Nunes FM, Rosário Domingues M, Coimbra MA. Demonstration of the presence of acetylation and arabinose branching as structural features of locust bean gum galactomannans. Carbohydrate Polymers. 2011;**86**:1476-1483. DOI: 10.1016/j.carbpol.2011.06.049

[37] Rizzo V, Tomaselli F, Gentile A, La Malfa S, Maccarone E. Rheological properties and sugar composition of locust bean gum from different carob varieties (Ceratonia siliqua L.). J. Agric. Food Chem. 2004;**52**:7925-7930. DOI: 10.1021/jf0494332

[38] Goycoolea FM, Morris ER, Gidley MJ. Viscosity of galactomannans at alkaline and neutral pH: evidence of 'hyperentanglement' in solution. Carbohydrate Polymers. 1995;**27**(1): 69-71. DOI:10.1016/0144-8617(95)00030-B

[39] Crescenzi V, Dentini M, Risica D, Spadoni S, Skjåk-Braek G, Capitani D, Mannina L, Viel S. C(6)-oxidation followed by C(5)-epimerization of guar gum studied by high field NMR. Biomacromolecules. 2004;**5**:537-546. DOI: 10.1021/bm034387k

[40] Grasdalen H, Painter TJ. NMR studies of composition and sequence in legume seed galac-tomannans. Carbohydr Res. 1980;**81**:59-66. DOI: 10.1016/S0008-6215(00)85677-3

[41] Shimahara H, Suzuki H, Sugiyama N, Nisizawa K. Isolation and characterization of oligosaccharides from an enzymic hydrolysate of konjac glucomannan. Agricultural and Biological Chemistry. 1975;**39**(2):293-299. DOI: 10.1080/00021369.1975.10861604

[42] Maeda M, Shimahara H, Sugiyama N. Detailed examination of the branched structure of konjac glucomannan. Agricultural and Biological Chemistry. 1980;**44**(2):245-252. DOI: 10.1080/00021369.1980.10863939

[43] Bourriot S, Garnier C, Doublier JL. Phase separation, rheology and microstructure of micellar casein-guar gum mixtures. Food Hydrocolloids. 1999;**13**:43-49. DOI: 10.1016/ S0268-005X(98)00068-X

[44] Crescenzi V, Dentini M, Risica D, Spadoni S, Skjåk-Braek G, Capitani D, Mannina L, Viel S. C(6)-oxidation followed by C(5)-epimerization of guar gum studied by high field NMR. Biomacro-molecules. 2004;**5**:537-546. DOI: 10.1021/bm034387k

[45] Barbucci R, Pasqui D, Favaloro R, Panariello G. A thixotropic hydrogel from chemically cross-linked guar gum: synthesis, characterization and rheological behavior. Carbohydrate Research. 2008;**343**(18):3058-3065. DOI: 10.1016/j.carres.2008.08.029

[46] Kato K, Matsuda K. Isolation of oligosaccharides corresponding to the branching-point of konjac mannan. Agricultural and Biological Chemistry. 1973;**37**(9):2045-2051. DOI: 10.1080/ 00021369.1973.10860944

[47] Kato K, Matsuda K. 1969. Studies on the chemical structure of konjac mannan Part I. isolation and characterization of oligosaccharides from the partial acid hydrolyzate of the mannan. Agr. Biol. Chern. 1969;**33**(10):1446-1453. DOI: 10.1080/00021369.1969. 10859484

[48] Shimahara H, Suzuki H, Sugiyama N, Nisizawa K. Isolation and characterization of oligosac-charides from an enzymic hydrolysate of konjac glucomannan. Agr. Biol. Chern. 1975;**39**(2):293-299. DOI: 10.1080/00021369.1975.10861604

[49] Maeda M, Shimahara H, Sugiyama N. Detailed examination of the branched structure of konjac glucomannan. Agric. BioI. Chem. 1980;**44**(2):245-252. DOI: 10.1080/00021369.1980. 10863939

[50] Cescutti P, Campa C, Delben F, Rizzo R. Structure of the oligomers obtained by enzymatic hydrolysis of the glucomannan produced by the plant Amorphophallus konjac. Carbohydrate Research. 2002;**337**(24):2505-2511. DOI: 10.1016/S0008-6215(02)00332-4

[51] Katsuraya K, Okuyama K, Hatanaka K, Oshima R, Sato T, Matsuzaki K. Constitution of kon-jac glucomannan: chemical analysis and 13C NMR spectroscopy. Carbohydrate Polymers. 2003;**53**:83-189. DOI: 10.1016/S0144-8617(03)00039-0

[52] Kato K, Matsuda K. Isolation of oligosaccharides corresponding to the branching-point of konjac mannan. Agr. BioI. Chem. 1973;**37**(9):2045-2051. DOI: 10.1080/00021369.1973.10860944

[53] Tatirat O, Charoenrein S, Kerr WL. Physicochemical properties of extrusion-modi?ed konjac glucomannan. Carbohydrate Polymers. Iowa, USA, 2012;**87**:1545-1551. DOI: 10.1016/j.carbpol.2011.09.052

[54] Ratcliffe I, Williams PA, English RJ, Meadows J. Small stain deformation mesurements of kon-jac glucomannan solutions and influence of borate cross-linking. Carbohydrate Polymers. Cambridge, UK, 2013;**95**:272-281. DOI: 10.1016/j.carbpol.2013.02.024

[55] Chudzik B, Zarzyka B, Śnieżko R. Immunodetection of arabinogalactan proteins in different types of plant ovules. Acta Biologica Cracoviensia Series Botanica. 2005;**47**(1):139-146

[56] Mao CF, Klinthong W, Zeng YC, Chen CH. On the interaction between konjac glucomannan and xanthan in mixed gels: An analysis based on the cascade model. Carbohydrate Polymers. 2012;**89**:98-103. DOI: 10.1016/j.carbpol.2012.02.056

[57] Brenner T, Tuvikene R, Fang Y, Matsukawa S, Nishinari K. Rheology of highly elastic iota-carrageenan/kappa-carrageenan/xanthan/konjac glucomannan gels. Food Hydrocolloids. 2015;**44**:136-144. DOI: 10.1016/j.foodhyd.2014.09.016

[58] Dickinson E. Hydrocolloids at interfaces and the influence on the properties of dispersed systems. Food Hydrocolloids. 2003;**17**:25-39. DOI: 10.1016/S0268-005X(01)00120-5

[59] Akiyama Y, Eda S, Kat̄a K. Gum arabic is a kind of arabinogalactan-protein. Agric. Biol. Chem. 1984;**48**(1):235-237. DOI: 10.1080/00021369.1984.10866126

[60] Yadav MP, Igartuburu JM, Yan Y, Nothnagel EA. Chemical investigation of the structural basis of the emulsifying activity of gum arabic. Food Hydrocolloids.2007;**21**:297-308. DOI: 10.1016/j.foodhyd.2006.05.001

[61] Sharma A, Gautam S, Wadhawan S. Xanthomonas. In: Batt CA, Tortorello ML, editors. Encyclopedia of Food Microbiology. Academic Press is an imprint of Elsevier; 2014. pp. 811-817

[62] Smith F. The constitution of arabic acid. Part I. The isolation of 3-d-galactosido-1-arabinose. J Chem Soc. 1939;744-753. DOI: 10.1039/JR9390000744

[63] Williams PA, Phillips GO 2000. Introduction to food hydrocolloids w: Handbook of hydrocol-loids Edited by Phillips GO, Williams PA. Woodhead Publishing Limited

[64] Chudzik B, Zarzyka B, Śnieżko R. Immunodetection of arabinogalactan proteins in differenttypes of plant ovules. Acta Biologica Cracoviensia Series Botanica. 2005;**47**(1): 139-146

[65] Nieto MB, Akins M. Hydrocolloids in bakery fillings. In: Laaman TR, editor. Hydrocolloids in Food Processing. Blackwell Publishing. Ltd. and Institute of Food Technologists; 2011

[66] Showalter A. M. Arabinogalactan-proteins: structure, expression and function. CMLS Cellular and Molecular Life Sciences. 2001;**58**:139-141. DOI: 10.1007/PL00000784

[67] Islam AM., Phillips GO, Sljivo A, Snowden MJ, Williams PA. A review of recent developmenton the regulatory, structural and functional aspects of gum arabic. Food Hydrocolloids. 1997;**11**(4):493-505. DOI:10.1016/S0268-005X(97)80048-3

[68] Dickinson E. Hydrocolloids at interfaces and the influence on the properties of dispersed sys-tems. Food Hydrocolloids. 2003;**17**:25-39. DOI:10.1016/S0268-005X(01)00120-5

[69] Ratcliffe I, Williams PA, Viebke C, Meadows, J. Physicochemical characterization of konjac glucomannan. Biomacromolecules. 2005;**6**(4):1977-1986. DOI: 10.1021/bm0492226

[70] Harding NE, Ielpi L, Cleary JM. 1995. Genetics and biochemistry xanthan gumproduction by Xanthomonas campestris w: Food Biotechnology Microorganisms. editors Hui YH, Khachatourians GC. VCH Publishers. New York. pp. 495-514

[71] Sharma A, Gautam S, Wadhawan S. Xanthomonas w: Encyclopedia of Food Microbiol-ogy Editor-In-Chief Batt CA Editor Tortorello ML Academic Press is an imprint of Elsevier. 2014 Elsevier. 811-817

[72] Jansson PE, Keene L, Lindberg B. Structure of the exocellular polysaccharide from Xanthomonas campestris. Carbohydr Res. 1975;**45**:275-282. DOI: 10.1016/S0008-6215(00) 85885-1

[73] Melton LD, Mindt L, Rees DA, Sanderson GR. Covalent structure of the polysaccharide from Xanthomonas campestris: evidence from partial hydrolysis studies. Carbohydrate Research. 1976;**46**(2):245-257. DOI: 10.1016/S0008-6215(00)84296-2

[74] Al-Assaf S, Phillips GO, Williams PA. Studies on acacia exudate gums. Part I: the molec-ular weight of Acacia senegal gum exudates. Food Hydrocolloids. 2005;**19**:647-660. DOI: 10.1016/j.foodhyd.2004.09.002

[75] Viebke C, Piculell L, Nilssont S. On the mechanism of gelation of helix-forming biopoly-mers. Macromolecules. 1994;**27**:4160-4166. DOI: 10.1021/ma00093a017

[76] Dua B, Lia J, Zhanga H, Huangb L, Chenb P, Zhoub J. Influence of molecular weight and degree of substitution of carboxymethylcellulose on the stability of acidified milk drinks. Food Hydrocolloids. 2009;**23**(5):1420–1426. DOI: 10.1016/j.foodhyd.2008.10.004

[77] Shakun M, Maier H, Heinze T, Kilz P, Radke W. Molar mass characterization of sodium car-boxymethyl cellulose by SEC-MALLS. Carbohydrate Polymers. 2013;**95**:550–559. DOI: 10.1016/j.carbpol.2013.03.028

[78] Viebke C, Piculell L, Nilssont S. On the Mechanism of Gelation of Helix-Forming Bio-polymers. Macromolecules. 1994;**27**:4160-4166. DOI: 10.1021/ma00093a017

[79] Viebke C, Williams PA. Determination of molecular mass distribution of κ-carrageenan and xanthan using asymmetrical flow field-flow fractionation. Food Hydrocolloids. 2000;**14**:265–270. DOI:10.1016/S0268-005X(99)00066-1

[80] Dea ICM, Morrison A. Chemistry and interactions of seed galactomannans. Advances in Carbohydrate Chemistry and Biochemistry 1975;**31**:241-312. DOI: 10.1016/S0065-2318(08)60298-X

[81] Bourriot S, Garnier C, Doublier JL. Phase separation, rheology and microstructure of micellar casein-guar gum mixtures. Food Hydrocolloids. 1999;**13**:43-49. DOI: 10.1016/S0268-005X(98)00068-X

[82] Barbucci R, Pasqui D, Favaloro R, Panariello G. A thixotropic hydrogel from chemically cross-linked guar gum: synthesis, characterization and rheological behavior. Carbohydrate Research. 2008;**343**(18):3058-3065. DOI: 10.1016/j.carres.2008.08.029

[83] Ratcliffe I, Williams PA, English RJ, Meadows J. Small stain deformation mesurements of konjac glucomannan solutions and influence of borate cross-linking. Carbohydrate Polymers. 2013;**95**:272-281. DOI: 10.1016/j.carbpol.2013.02.024

[84] Cuvelier G, Launay B. Concentration regimes in xanthan gum solutions deduced from flow and viscoelastic properties. Carbohydrate Polymers. 1986;**6**:321-333. DOI: 10.1016/0144-8617(86)90023-8

[85] Smith F. The constitution of arabic acid. Part I. The isolation of 3-d-galactosido-1-arabi-nose. Journal of the Chemical Society. 1939;744-753. DOI: 10.1039/JR9390000744

[86] Viebke C, Williams PA. Determination of molecular mass distribution of κ-carrageenan and xanthan using asymmetrical flow field-flow fractionation. Food Hydrocolloids. 2000;**14**:265-270. DOI: 10.1016/S0268-005X(99)00066-1

[87] Kishida N, Okimasu S, Kamata T. Molecular weight and intrinsic viscosity of konjac gluco-mannan. Agric. Biol. Chem. 1978;**42**(9):1645-1650. DOI: 10.1080/00021369.1978.10863226

[88] Kishida N, Okimasu S, Kamata T. Molecular weight and intrinsic viscosity of konjac glucomannan. Agricultural and Biological Chemistry. 1978;**42**(9):1645-1650. DOI: 10.1080/00021369.1978.10863226

[89] Xiaoyan L, Qiang W, Xuegang L, Feng L, Xiaoqing L, Pan H. Effect of degree of acetyla-tion on thermoplastic and melt rheological properties of acetylated konjac glucomannan. Carbohydrate Polymers. 2010;**82**:167-172. DOI: 10.1016/j.carbpol.2010.04.053